# 4. Discussion

## 4.1 Role of the STAT1 N-domain in nuclear import and dephosphorylation

Nuclear import of STATs is crucial to their function as transcription factors and significant progress has been made in the last few years considering our understanding of how STATs gain access to their target genes (McBride and Reich, 2003; Vinkemeier, 2004; Meyer and Vinkemeier, 2004). Upon tyrosine phosphorylation, STAT1 exposes a dimer-specific nuclear import signal (dsNLS, Meyer et al., 2002a). This signal, which is located in the DNA binding domain, is necessary for the formation of a transport complex with importin-α5 (McBride et al., 2002; Fagerlund et al., 2002). Also the N-domain has been implicated in nuclear translocation of STATs, since N-terminally truncated mutants did not accumulate in the nucleus of cells following cytokine stimulation (Strehlow and Schindler, 1998). However, the authors did not differentiate between a nuclear import or a nuclear retention defect (see 1.4.2), which both could explain a loss of nuclear accumulation of the transcription factor.

In the present work we demonstrated that the STAT1 N-domain is required for importin-α5 binding in addition to the dsNLS in the DNA binding domain of the transcription factor (Fig. 3.6; Meissner et al., 2004b). The nuclear accumulation phenotype of N-terminal mutants of STAT1 can thus be attributed to defective nuclear import, rather than to impaired retention in the nucleus. Importin-α5 has been identified as the only import receptor for STAT1 (Sekimoto et al., 1997; Melen et al., 2003), and it has been revealed by gel filtration analysis that two importin-α5 molecules bind to an activated STAT1 dimer (Fagerlund et al., 2002), however, the contribution of the N-domain to the binding of importin-α5 has not been analysed. Using three complementary approaches we could rule out that the N-domain of STAT1 provides a conventional binding site for importin-α5 in the form of an autonomous, transferable NLS (Dingwall et al., 1982). Neither as a GFP fusion protein expressed in HeLa S3 cells (Fig. 3.2), nor in a microinjection assay (Fig. 3.3) the N-domain provided any evidence for the presence of transport activity. A requirement for post-translational modifications coming along with cytokine treatment could be excluded, since interferon stimulation did not influence the distribution of the N-domain expressed in HeLa S3 cells (data not shown). In a third approach we examined the full length protein for the contribution of positively charged surface residues to nuclear import. The N-domain of STAT1 has at least two surface-exposed clusters of positively-charged residues that resemble monopartite NLSs (Dingwall et al., 1982). However, alanine mutation of single ($K^{13}$, $R^{70}$) or multiple charged

surface residues ([$H^{81}$, $R^{84}$, $K^{85}$, $R^{88}$][$K^{110}$, $E^{111}$, $R^{113}$, $K^{114}$]), covering these regions, did not interfere with the nuclear accumulation behaviour of the respective STAT1 mutant proteins (Figs. 3.4 and 3.5).

In our initial analysis, the only mutation of a charged residue that interfered with nuclear accumulation was $R^{31}A$. However, it was realised before that the protein is destabilised by the mutation (Shuai et al., 1996), which is likely to be explained by the central role of this residue in maintaining the ring-shaped element that constitutes a major part of the N-domain (Vinkemeier et al., 1998). In accordance with the crystal structure, we demonstrate here that mutations of structurally important residues all result in identical phenotypes that entail loss of nuclear accumulation, N-terminal degradation, and defective tyrosine dephosphorylation (see Figs. 3.8, 3.9 and 3.10). Of note, the residues in question [$Trp^4$, $Trp^{37}$, $Glu^{39}$, $Glu^{112}$] are invariant in all mammalian STAT protein family members, as is $Arg^{31}$ (Fig. 1.4). Remarkably, mutation of neighbouring side chains that do not fulfil obvious structural functions was either without phenotypical consequences [$Glu^{111}$], or resulted specifically in defective tyrosine dephosphorylation, whereas nuclear import remained normal [$Phe^{77}$, see below (Meyer et al., 2004)]. Furthermore, the isolated N-domain with a mutation of $R^{31}A$ was unstable or expressed predominantly as an insoluble aggregate (Fig. 3.11). Similar observations were made for the N-domain harbouring the mutation $Trp^{37}$ (Chen et al., 2003). These results indicated that mutation of structurally important residues, such as arginine 31, caused an overall destabilisation of the N-domain. Concomitant functional defects are therfore not site-specific. We predict that disruption of the N-domain architecture is likely to prevent the formation of a functional import complex of STAT1 and transport factors. Direct binding to the $R^{31}A$ mutant protein, however, could not be analysed, due to the low expression and instability of the mutant protein.

The residue arginine 31 was also suggested to be involved in phosphatase recruitment (Shuai et al., 1996), and several studies made use of a STAT1 mutant where arginine 31 was replaced by alanine to investigate the physiological role of tyrosine dephosphorylation. It was shown that the mutation resulted in prolonged tyrosine phosphorylation and enhanced antiproliferative activity of both type I and II IFN (Shuai et al., 1996; Mowen et al., 2001). These observations, however, only provided indirect evidence supporting the involvement of $R^{31}$ in phosphatase recruitment. Direct binding or loss of binding of STAT1 to the nuclear phosphatase upon mutation of $Arg^{31}$ to alanine has not been demonstrated. The results presented in this thesis strongly argue against a direct role of $R^{31}$ in phosphatase recruitment. As outlined above, mutation of $R^{31}$ destabilises the N-domain. Moreover, we demonstrated

here that the dephosphorylation defect is not restricted to mutation of arginine 31 to alanine, but is shared by all other mutations [$Trp^{4}$, $Trp^{37}$, $Glu^{39}$, $Glu^{112}$] that affect the structural integrity of the STAT1 N-domain (Fig 3.9). Our results suggest that the hyperphosphorylation phenotype of STAT1ΔN and of the $R^{31}A$ mutant - similar to the import defect - may rather be caused by an overall destabilisation of the N-domain.

It remains controversial, to what extent the import defect of N-terminal mutants contributes to the observed hyperphosphorylation phenotype. STATs get inactivated predominantly in the nucleus (Haspel et al., 1996; Haspel and Darnell, 1999), and the finding that N-terminal mutants of STAT1 do not enter the nucleus could well explain the impaired dephosphorylation. However, there is also considerable phosphatase activity in the cytoplasm, and several cytoplasmic phosphatases have been described to dephosphorylate STATs (Aoki and Matsuda, 2000; Simoncic et al., 2002; Wu et al., 2002). Moreover, the nuclear isoform of the TC-PTP has recently been shown to shuttle between the cytoplasm and the nucleus (Lam et al., 2001). Thus, the nuclear import defect alone is rather unlikely to account for the hyperphosphorylation phenotype. Yet, further investigation will be required to distinguish between the nuclear import defect and defective phosphatase recruitment as a cause of the impaired dephosphorylation of N-terminal mutants. Preliminary data from our group, shows that STAT1ΔN is not dephosphorylated by TC45 *in vitro* (Thomas Meyer, unpublished data). Also microinjection of recombinant, *in vitro*-phosphorylated STAT1ΔN into the nuclei of cells, with subsequent monitoring of the dephosphorylation kinetics will help to address this question.

A recent analysis of STAT1 tyrosine dephosphorylation has provided new evidence for a contribution of the STAT1 N-domain in phosphatase recruitment. Meyer et al. (2004) identified a surface residue in helix 7, which seems to be required for association with the phosphatase TC45. While mutation in STAT1 of phenylalanine 77 ($Phe^{81}$ in STAT5) to alanine prevented tyrosine dephosphorylation, the nuclear import behaviour of the mutant was not changed. In agreement with previous findings that only unphosphorylated STAT1 is able to leave the nucleus (Meyer et al., 2003), the mutant protein $F^{77}A$ showed a prolonged nuclear presence. Furthermore, the mutation $F^{77}A$ could rescue the accumulation defect of DNA binding mutants, underlining the importance of dephosphorylation for nuclear export of STAT1. So far $F^{77}A$ is the only mutation that can separate the two functions: The mutant protein has a dephosphorylation defect despite intact nuclear import behaviour.

The results obtained with STAT1 in this study can only partially be applied to other STAT family members, since the N-domains seem to have common but also distinct

functions. The average sequence identity between the different STAT N-domains is ~40% and ranges between 51% between STAT1 and STAT4 to 20% between STAT5 and STAT6. However, despite the high sequence identity, the N-domains of STAT1 and STAT4 seem to operate differently. Contrary to STAT1, the N-domain of STAT4 was reported to be required for dimerisation and receptor-mediated phosphorylation (reviewed in Berenson et al., 2004). STAT4ΔN can be phosphorylated *in vitro* (Xu et al., 1996), however, *in vivo* deletion of the N-domain abolished receptor association and subsequent activation by IL-12 (Murphy et al., 2000; Chang et al., 2003; Ota et al. 2004). Similar to STAT4, also truncations of the STAT2 N-domain (Δ59) prevented tyrosine phosphorylation of STAT2 (Qureshi et al., 1996) and the N-domain of STAT2 has therefore been suggested to be engaged in association with the IFNα receptor (Li et al., 1997). More recently, however, receptor association prior to cytokine stimulation has been demonstrated to be independent of the first 135 amino acids of STAT2 (Nguyen et al., 2002).

Sequence similarity may represent a better indicator of common functions, since they are likely to be encoded by surface residues that are less conserved than the residues maintaining the N-domain structure (Fig 1.4). A family tree, which depicts the relatedness of the different STAT N-domains on the basis of sequence similarity, places STAT1 and STAT3 in close proximity (Fig. 4.1), and indeed the two STAT family members seem to make use of their N-domains in a similar way. STAT3 lacking the N-domain (STAT3ΔN) was found to be constitutively phosphorylated on $Tyr^{705}$ in HepG2 cells (Zhang et al., 2000), pointing out a similar role of the STAT3 N-domain in dephosphorylation as described here for the N-domain of STAT1. Furthermore, similar to STAT1, STAT3 does not require the N-domain for sufficient activation via IL-6 or EGF stimulation (Zhang et al., 2000), and mutations that have been described to abolish tetramer formation of STAT3 ($W^{37}A$, $Q^{66}A$) did not interfere with the IL-6-induced phosphorylation of STAT3, or binding to a single GAS site (Zhang and Darnell, 2001). Also the N-domain of STAT5 seems to fulfil similar functions to the N-domain of STAT1. Deletion of the first 136 amino acids of STAT5 did not affect IL-3 induced tyrosine phosphorylation (Wang et al., 2000) and, moreover, a nuclear accumulation defect has been observed for STAT5b. N-terminal truncation mutants (Δ104, Δ138, Δ165) did not accumulate in the nucleus upon IL-3 stimulation (Zeng et al., 2002). The role of the STAT6 N-domain in dephosphorylation is more controversial. A naturally occurring splice variant has been described for STAT6 (Δ110, Patel et al., 1998), and it was demonstrated that STAT6Δ110 gets phosphorylated in response to IL-4, yet, to a lesser extent than the wild

type. However, recently, it has been reported that mutation of $Arg^{27}$ of STAT6 to alanine resulted in reduced expression and in loss of activation and DNA binding (Chen et al., 2004).

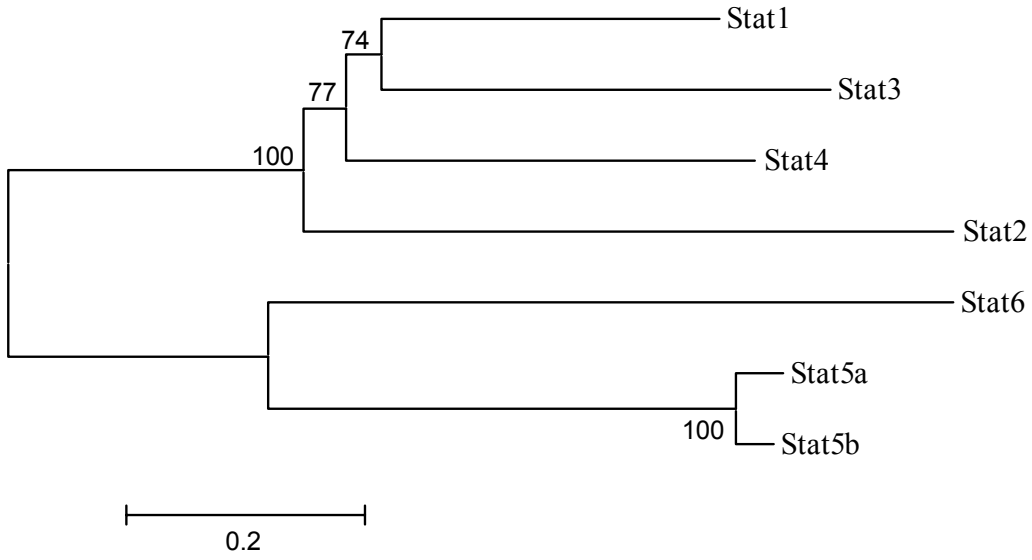


**Fig. 4.1** Similarity tree showing the sequence homology between the N-terminal domains of human STATs. The sequence alignment was prepared with ClustalW 1.8 as described for Fig. 1.4 and depicted as dendrogram with MEGA 2.0. Numbers at diverging branches show the reliabilities of these branches based on bootstrap resampling. The scale underneath the tree describes the Poisson correction distance based on the number of amino acid substitutions per site.

In summary, we have demonstrated the importance of structurally conserved residues in maintaining an import-, and dephosphorylation-competent conformation of the STAT1 N-domain. While structurally important residues are well conserved between the different STATs (Figs. 1.3 and 1.4), surface-exposed residues are less conserved and surely account for the functional differences between single STAT family members. An extended mutagenesis of the surface residues of the STAT N-domains will help to understand how the diverse functions get integrated on the surface of the N-domain.

## 4.2 Arginine methylation of STAT1 does not determine the interferon insensitivity of tumor cells

It was previously reported that arginine methylation of the transcription factor STAT1 is a crucial determinant of the biological activities of IFNα (Mowen et al., 2001). The data presented in this thesis contradict that model. Extensive mass spectrometric analyses of

STAT1 isolated from untreated as well as from IFNα or -γ-stimulated cells failed to provide evidence for methylation of residue arginine 31. MALDI-MS analysis as well as nanoLC-ESI-MS/MS readily demonstrated the presence of non-methylated peptides covering $Arg^{31}$, but we did not detect the respective modified fragments (Fig. 3.15A). In the original report by Mowen and co-authors (2001) mass spectrometry data was reported without providing sequencing data for peak identification and without negative controls. Standing alone, the fact that peptides with the appropriate mass were identified is no proof of arginine methylation of STAT1. The argumentation, methylated peptides went undetected in our analysis due to insufficient ionisation could be ruled out by comparing the detection of synthetic $R^{31}$ unmethylated and $R^{31}$ dimethylated peptides. MALDI and ESI measurements yielded comparable ion intensities irrespective of methylation (Figs. 3.15B and 3.16C). Moreover, in this and the study of Mowen and co-authors (2001) isoschizomeric enzymes were used to exclude variations in the generation of peptides as a cause for differences in the subsequent MALDI analysis. A possible cause of variability could rest with the cells that were used. For mass spectrometric analyses we purified STAT1 from stably reconstituted U3A cells. Yet, U3A cells are derived from 2fTGH cells that were reported to contain ample amounts of methylated STAT1 (Mowen et al., 2001).

In the original report on the arginine methylation of STAT1 the argumentation hinges on a novel immunoprecipitation assay (Mowen and David, 2001). A monoclonal antibody directed against dimethylarginine was employed and the precipitate was demonstrated to contain STAT1 (Mowen et al., 2001). However, while this antibody can precipitate methylated proteins, it cannot be used in Western blotting experiments to directly confirm the presence of methyl-groups in an isolated protein preparation (Mowen and David, 2001). Hence, this approach does not prove methylation of a specified target protein, since co-precipitation of non-methylated proteins cannot be ruled out. Unfortunately, the work of Mowen and co-authors (2001) has mislead others in their interpretation: arginine methylation of STAT3 and STAT6 was reported (Rho et al., 2001; Chen et al., 2004). Yet, the authors of both studies do not provide any other evidence for arginine methylation by other means than the unspecific immunoprecipitation approach.

Here, *in vivo* labelling of endogenous proteins with the methyl-donor L-[*methyl*-$^{3}$H]methionine followed by immunoprecipitation with specific STAT1 antibodies and fluorography was used. While we observed methylation of a number of cellular proteins, the STAT1 precipitate, which was confirmed by Western blotting and silver staining, did not contain detectable quantities of radioactive STAT1 in two independent experiments. The *in*

*vivo* labelling experiments performed in this study were done with HeLa cells (Fig. 3.17), which were previously described to contain methylated STAT1 (Mowen et al., 2001). For these reasons we consider cell type-specific differences an unlikely cause for the discrepancies. Therefore, we conclude that STAT1 is not the target of trans-methylation reactions to a relevant extent.

Mowen and co-authors (2001) used the $R^{31}A$ mutant to study the functional consequences of arginine methylation and reported enhanced transcriptional activity upon stimulation with interferon alpha. Central to their interpretation is the claim that the mutation of arginine 31 to alanine mimics arginine methylation of STAT1. The results presented in this thesis strongly argue against this model. Our mutational analysis clearly revealed a role of arginine 31 in maintaining the structural integrity of the N-domain, as suggested by the crystal structure, and the $R^{31}A$ mutant protein displayed serious functional defects. It was realised before that mutation of $Arg^{31}$ to alanine destabilises the protein (Shuai et al., 1996) and, similarly, mutation of the homologous $Arg^{27}$ to alanine in STAT6 resulted in a 10 fold decrease of expression and increased degradation of the mutant protein (Chen et al., 2004). Moreover, the $R^{31}A$ mutant protein displayed a similar nuclear import and dephosphorylation defect as observed upon deletion of the whole N-domain (Figs. 3.8 and 3.9). In their study, Mowen et al. (2001) made use of a stabilised version of $R^{31}A$ as a C-terminal fusion to GST. In agreement with previous reports, we observed that indeed the protein is stabilised (Shuai et al., 1996; Mowen et al., 2001). Yet, fusion of $R^{31}A$ to GST neither rescued the dephosphorylation phenotype nor restored nuclear import of the mutant protein (Figs. 3.12 and 3.13). Given the nuclear translocation defect, the mutant STAT1 derivative expectedly was not capable to activate an IFNα-responsive reporter gene, while wild type STAT1 fused to GST did. Again, these results contradict previous data with the $R^{31}A$ mutant of STAT1, where enhanced IFNα-induced transcription was reported (Shuai et al., 1996; Mowen et al., 2001). However, those data were collected in cells that express endogenous STAT1 protein. It has previously been reported that wild type STAT1 can rescue the translocation phenotype of N-terminal mutants (Strehlow and Schindler, 1998), thus making it impossible to discern transcriptional activity of the mutant from mere interference with the wild type protein. Our results obtained in U3A cells, which do not express endogenous STAT1, unambiguously demonstrate that the $R^{31}A$ mutant of STAT1 is incapable to transmit cytokine signals into the cell nucleus, and that it therefore does not constitute a valid model for the transcriptional functions of STAT1.

Loss of function upon mutation of the N-domain, in a STAT1-deficient background, is not without precedence. U3A cells complemented with STAT1ΔN displayed no IFNγ-induced up-regulation of MHC-I, which is observed upon transfection with wild type STAT1 (Meraz et al., 1996). In addition, our results are supported by the characterisation of the first STAT1 knock-out mice (Meraz et al., 1996). Due to initiation of transcription at the internal methionine 135, small amounts of N-terminally truncated STAT1 were produced. Yet, the mice lacked responsiveness to interferons and were highly sensitive to microbial pathogens and to viral infection (Meraz et al., 1996), once more indicating that STAT1ΔN is not functional. In *Drosophila melanogaster* alternative promotor use generates a naturally occurring isoform of STAT92E lacking the N-terminal 133 amino acids, and the resulting STAT92EΔN has been described to act as a dominant-negative inhibitor in JAK-STAT signalling during embryonic development (Henriksen et al., 2002).

A central argument in support of arginine methylation of STAT1 was the observation that treatment of cells with the methyltransferase inhibitor 5'-deoxy-5'-methylthioadenosine (MTA) inhibited DNA binding of STAT1 while tyrosine phosphorylation was not altered. The loss of DNA binding and the diminished transcription were attributed to the facilitated interactions of non-methylated STAT1 with the inhibitor PIAS1 (Mowen et al., 2001; Duong et al., 2004). However, our results concerning the effects of MTA on STAT1-dependent gene activation differ strongly, and hence do not support this model. First, we cannot confirm that tyrosine phosphorylation and DNA binding are uncoupled after MTA treatment. Rather, reduced DNA binding correlated with reduced tyrosine phosphorylation (Fig. 3.21). Similar observations were also made for STAT6 (Chen et al. 2004). Importantly, MTA exerted its effects on STAT1 phosphorylation even in the absence of the STAT1 N-domain (Fig. 3.22), ruling out a contribution of $Arg^{31}$. Second, MTA also affected tyrosine dephosphorylation reactions, as the low level of STAT1 phosphorylation seen after IFNα-stimulation persisted longer than in untreated cells (Fig. 3.23). In addition, the effects of MTA are not interferon- or STAT-specific, since the TNFα-induced serine phosphorylation of the MAP kinase p38 was also prolonged by MTA (Fig. 3.24). Also, MTA negatively influenced STAT1-independent gene transcription. This is demonstrated by the loss of NF-κB-dependent reporter gene activity in response to TNFα (Fig. 3.19). We therefore concluded that MTA is an unspecific inhibitor of multiple enzyme reactions and various signalling pathways. Keeping in mind that MTA is known to impact a wide range of cellular processes, many of which directly or indirectly influence transcriptionally regulated processes such as cell growth (Garcia-Castellano et al., 2002; Kamatani and Carson, 1980; Kubota et al., 1985), these results are not

entirely surprising. Generally MTA is therefore not considered to be a specific inhibitor of transmethylation reactions, since it also leads to perturbations of spermine synthesis, ornithine decarboxylation and other biosynthetic pathways (Pajula and Raina, 1979; Kamatani and Carson, 1980; Raina et al., 1982; Kubota et al., 1985; Carson et al., 1988; Maher, 1993). It is obvious from the above that the association of STAT1 with its inhibitor PIAS1 is not regulated by methylation, and currently no alternative model exists that describes their molecular interaction. Therefore, it remains unexplained how the PIAS proteins exert their proposed specificity in modulating JAK-STAT signalling.

The work of Mowen and contributors (2001) has also gained significant attention, because of the direct clinical relevance of their findings. It was reported that lung carcinoma cells that lack the enzyme methylthioadenosine phosphorylase (MTAP), and thus accumulate the methyltransferase inhibitor MTA, show an impaired response to IFNα. The authors proposed the model that the insensitivity of such tumor cells to IFN therapy may be explained by a lack of STAT1 arginine methylation due to excess amounts of MTA. According to their model, reconstitution of MTAP-deficient cells with the functional enzyme should revert their interferon insensitivity. Yet, in our hands reconstitution of MTAP-deficient breast cancer cells did not increase IFNα-mediated transcription (Fig. 3.25). To reduce MTA breakdown in the culture medium, in some experiments fetal calf serum was replaced by 10% horse serum, which lacks MTAP activity (Kamatani et al., 1981). However, we did not note differences between cells growing in medium supplemented with fetal calf serum or horse serum. Cell type-specific differences may contribute to the differential MTAP sensitivity. Still, our results argue against a general functional link between MTAP deficiency and STAT1 signal transduction.

In summary, our examination of STAT1 arginine methylation provided evidence that contradicts previous results that stated methylation of residue $Arg^{31}$. The alanine mutation of $Arg^{31}$, which was considered to functionally mimic the arginine methylated protein, is demonstrated to result in structural perturbations with unspecific functional consequences. Moreover, methylthioadenosine is revealed to modulate multiple signalling pathways, irrespective of whether STAT1 is involved or not. Thus, alternative explanations to STAT1 methylation need to be explored in order to understand the molecular mechanisms that underlie the reduced interferon sensitivity of many tumor cells.

## 4.3 Ratjadone A - a new tool to study CRM1-dependent nuclear protein export

Ratjadone A was originally isolated from the myxobacterium *Sorangium cellulosum* as a secondary metabolite with antifungal activity (Gerth et al., 1995) and it was later shown to inhibit the growth of mammalian cell lines (Burzlaff et al., 2003). Its similar structure to the well-characterised export inhibitor leptomycin B (LMB, see Fig 1.6) suggested that both drugs may act through a common reaction mechanism. Using two different protein export assays we demonstrated here that ratjadone A indeed inhibits nuclear export in an identical way to LMB. We first showed that ratjadone A can block the cytoplasmic accumulation of an NES-containing export reporter protein expressed in HeLa S3 cells (GFP-NES, Fig. 3.27). Nuclear export signals are leucine-rich, loosely conserved consensus sequences that are recognised by the export receptor CRM1 (la Cour et al., 2003). To demonstrate that indeed nuclear export was affected, we employed a second export assay. We injected a recombinant reporter protein (GST-NES-GFP) directly into the nuclei of HeLa S3 cells and analysed its nuclear export kinetics in the absence or presence of LMB and ratjadone A. Again, the cytoplasmic accumulation of the reporter protein was inhibited by both drugs at a identical concentration (10 ng/ml, Fig. 3.28). The microinjection assay clearly revealed that a nuclear export block was responsible for the prolonged nuclear presence of the export reporter GST-NES-GFP. Alternative explanations such as an increased nuclear import of the reporter protein or a drug-induced disruption of the nuclear membrane could thus be excluded. Our results are in agreement with the findings of Köster and co-authors (2003) who observed that ratjadone A inhibited nuclear export of NES-containing proteins in different cell lines. The authors also observed an enlargement of the nuclei of mouse L292 cells, which were cultivated over a period of 5 days in the presence of ratjadone. A similar increase in the size of nuclei from 70 $\mu m^2$ to a limiting value of 240 $\mu m^2$ was seen when the cells were treated with LMB indicating that the effects of the two drugs are comparable. Moreover, the enlargement of the nuclei correlated with the growth inhibitory properties of both LMB and ratjadone A suggesting a functional link between the observed export block and the cytotoxic effects of the two drugs.

It has previously been shown that LMB inhibits nuclear protein export by directly targeting the export receptor CRM1 (Kudo et al., 1998 and 1999). LMB binds covalently via its α,β-unsaturated δ-lactone to the sulfhydryl group of a conserved cysteine in the central conserved region (CCR) of CRM1 (Kudo et al., 1999). Similar to LMB, the polyketide ratjadone A possesses a terminal α,β-unsaturated δ-lactone and direct binding of ratjadone to

CRM1 has recently been reported (Köster et al., 2003). However, the mechanism by which the ratjadones inactivate CRM1 was not resolved. Using two complementary approaches, we demonstrated in this study that ratjadone A indeed uses the same reaction mechanism as LMB to inactivate CRM1. First, using mass spectrometry we confirmed the covalent binding of ratjadone A to $Cys^{528}$ of a synthetic peptide covering the conserved hydrophobic amino acids in the N-terminal flanking region of $Cys^{528}$ (residues 513-530). The sequence of the additional mass peak in the sample reacted with ratjadone A (Fig 3.29) and the position of ratjadone modification was confirmed by tandem MS. In addition, we demonstrated that mutation of the critical cysteine residue in human CRM1 ($Cys^{528}$) to serine rendered CRM1 insensitive to ratjadone A *in vivo*. Expression of the CRM1 mutant ($C^{528}S$) but not of the wild type protein rescued the observed export block in the presence of LMB and ratjadone A to a similar extent (Fig. 3.30). Our results are consistent with previous studies in yeast and human cell lines, which analysed the export inhibitory properties of LMB. Kudo and others (1999) showed that mutation of the homologous $Cys^{529}$ of CRM1 in *S. pombe* rendered the fission yeast resistant to the export inhibitory effects of LMB, and, conversely, mutation of $Thr^{539}$ in *Sac. cerevisiae*, which displayed LMB-resistance, to cysteine rendered the organism sensitive to LMB (Neville and Rosbash 1999). Overexpression of the human CRM1($C^{528}S$) mutant has been demonstrated to rescue the LMB-induced nuclear accumulation of the latent NF-κB/IκB complex in Hek cells (Huang et al., 2000). We concluded from the above that LMB and ratjadone A inhibit CRM1 via alkylation of the same conserved cysteine residue.

The central conserved region of CRM1 (aa 415-600) has been implicated in the RanGTP-dependent NES recognition (Ossareh-Nazari and Dargemont, 1999). However, whether $C^{528}$ directly participates in the binding of NES-containing export substrates was not clarified. In the fission yeast, the homologous residue $C^{529}$ itself appears to be non-essential for CRM1 function, and it can be replaced by Ser or Thr (Kudo et al., 1999; Neville and Rosbash, 1999). Askjaer and colleagues (1998) observed that a more C-terminal region of CRM1, encompassing residues 716-810, is involved in binding to the HIV Rev protein. Yet, this interaction did not rely on an intact NES sequence and was not LMB-sensitive. Two different models may explain the inhibitory effect of ratjadone A on NES binding: It may sterically block the NES binding site, or it may interfere with the conformation required for NES binding. Indeed, a significant mobility shift of the CRM1 protein in native gels was observed upon LMB treatment, suggesting that alkylation at the cysteine in the CCR alters the three-dimensional structure of the protein (Fornerod et al., 1997). A puzzling feature remained the specificity of this covalent modification. How can the two drugs modify a single

cysteine residue among the other cysteines in CRM1 and in other proteins? The amino acid cysteine is found with a frequency of 3.4% in proteins (Lathe, 1985), and human CRM1 contains 19 cysteine residues in addition to $Cys^{528}$. Moreover, cells contain high concentrations of glutathione (~5 mM GSH) and free L-cysteine which provide sulfhydryl groups that could potentially react with both drugs. Interestingly, LMB does not react with L-cysteine or GSH *in vitro* (Kudo et al., 1999) and it is conceivable that hydrophobic interactions with the CCR contribute to the high affinity of LMB/ratjadone A to CRM1. This idea is supported by our peptide labelling experiments. The formation of the covalent adduct *in vitro* required millimolar concentrations of ratjadone A, much higher than that for the *in vivo* binding to CRM1 (10 nM). Moreover, shortening of the hydrophobic acyl chain reduced the activity of both drugs (Kudo et al., 1999; Kalesse et al., 2001), favouring a model wherein LMB or ratjadone A bind to a hydrophobic pocket, which may also be responsible for the binding of the hydrophobic NES.

New evidence that the two polyketides ratjadone A and LMB prevent binding of NES-containing cargos to CRM1 comes from the recently proposed structure of human CRM1 (Petosa et al., 2004). The structure is based on the crystal structure of the C-terminal part of CRM1 and homology modelling of the N-terminal region to related karyopherins of the importin-β family of transport receptors. The structure predicts that the CRM1 residues involved in NES binding ($Leu^{525}$, $Lys^{568}$, and $Phe^{572}$) are in close vicinity to the critical cysteine residue 528, which could be confirmed by mutational analysis. According to this structural model, covalent attachment of LMB to $Cys^{528}$ sterically hinders access to the NES binding site. Furthermore, the structure also provides an explanation for the co-operative binding of RanGTP and NES containing export substrates. The RanGTP-binding loop was found to mask the cargo-binding pocket, and only a conformational change induced upon Ran and/or cargo binding allowed stable binding of RanGTP and cargo (Petosa et al., 2004). This also clarifies why preincubation of CRM1 with either ratjadone A or LMB blocked RanGTP and NES binding in a co-operative manner (Köster et al., 2003), and, conversely, why efficient LMB binding only occurred in the presence of RanGTP (Daelemans et al., 2005).

The ability of LMB to inhibit nuclear export has made it a useful tool in the study of the subcelluar distribution of a variety of proteins (Ossareh-Nazari et al., 2001). It has proven especially helpful in addressing the question of nucleocytoplasmic shuttling of proteins involved in signal transduction. Examples of proteins of which the shuttling between the cytoplasm and the nucleus has been revealed by the use of LMB are the MAPKK MEK1 (Fukuda et al., 1997), Smads (Xiao et al., 2001), and components of the NF-κB signalling

pathway, such as the inhibitor of NF-κB (IκB, Sachdev and Hannink, 1998; Huang et al., 2000), the NF-κB inducing kinase NIK, and IκB kinase1 (IKK1, Birbach et al., 2002). Furthermore, the use of LMB helped to identify targets of CRM1-dependent export which also comprise a variety of regulatory proteins such as cyclin B1 (Yang et al., 1998), MDM2/p53 (Freedman and Levine, 1998; Stommel et al., 1999). To prove the feasibility of ratjadone A in the study of protein nuclear export we extended our analysis to known CRM1-dependent export substrates. The CRM1-dependent relocalisation of STAT1 following cytokine treatment and p65 cytoplasmic accumulation mediated by the NES activity provided by IκB (Figs. 3.31 and 3.32) were blocked to a similar degree as described before for LMB (Begitt et al., 2000; McBride et al., 2000; Arenzana-Seisdedos et al., 1997; Johnson et al., 1999; Huang et al., 2000). Moreover, both drugs acted at the same concentration (10 ng/ml). Our results suggest that the export inhibitors ratjadone A and LMB can be used interchangeably as a tool in the study of protein nuclear export (Meissner et al., 2004a). The major advantage of ratjadone A over LMB is that it can be synthesised (Bhatt et al., 2001; Kalesse et al., 2001), while the commercially available LMB needs to be isolated from *Streptomyces* cultures (Asscher et al., 2001). This can influence the activity of different lots provided by the manufacturer. The synthesis of ratjadone A makes it independent from such drawbacks. Furthermore, the synthesis allows to exploit the power of synthetic chemistry. Using synthetic diastereomers, Kalesse et al (2001) could convincingly show that the overall geometry of ratjadone A, as determined by the configuration at C10, is crucial for its binding to the export receptor CRM1. Also the contribution of the hydrophobic acyl chain of ratjadone A to the binding of the export receptor was analysed using synthetic derivatives of ratjadone A (Kalesse et al., 2001).

The use of ratjadone A as a therapeutic agent, however, will most likely suffer from the same drawbacks as described for LMB. In an attempt to exploit the antiproliferative activity in cancer therapy, LMB was used in a phase I clinical trial under the name ‘elactocin’ (Newlands et al., 1996). Due to severe neurotoxic side-effects its use was not recommended for further clinical studies. Even when LMB was discovered to inhibit the export of the HIV-Rev protein and to suppress HIV replication in primary human monocytes *in vitro,* no further attempts were undertaken to use LMB in HIV therapy (Wolff et al., 1997). In addition, it has been shown that LMB arrests the embryonic development of *Xenopus* at the neurula stage (Callanan et al., 2000). More recently, it has been demonstrated that nuclear entrapment of the BCR-ABL oncoprotein can be used as a therapeutic strategy to selectively kill chronic myeloid leukemia cells (Vigneri and Wang, 2001). The authors observed that a combination

of LMB and the kinase inhibitor STI571 induced apoptosis in the BCR-ABL transformed cells, and suggest this treatment to purge explanted bone marrow of chronic myeloid leukemia cells.

## 4.4 Contribution of CRM1-mediated export to the nucleocytoplasmic distribution of STATs in resting cells

During the course of this study we observed that ratjadone A and LMB also changed the distribution of STATs in resting cells (Figs. 3.33-35). Treatment of HeLa S3 cells with LMB changed the predominantly cytoplasmic localisation of STAT1-GFP in resting cells to a pancellular distribution. The results were confirmed for endogenous STAT1 (Fig. 3.33D) and also in a different cell line (3T3, Fig. 3.34) using ratjadone A as export inhibitor. The change in localisation upon the export block did not depend on phosphorylation, since the same results were obtained with the tyrosine mutant STAT1 ($Y^{701}F$), which cannot be phosphorylated (data not shown). These findings pointed for the first time towards a role of CRM1-mediated export in regulating the nucleocytoplasmic localisation of STAT1 in resting cells. Previously, CRM1-mediated export of STATs has only been studied in the context of termination of cytokine-induced accumulation and no effect of LMB on STAT1 localisation in resting cells was reported (Begitt et al., 2000; McBride et al., 2000). Yet, the effect on STAT1 localisation is subtle and LMB/ratjadone A treatment did not lead to a readily detectable nuclear accumulation as observed for STAT3 (Fig. 3.35). The more drastic effect of LMB on the localisation of STAT3 has in the meantime been observed by several other groups (Bhattacharya and Schindler, 2003; Ma et al., 2003; Pranada et al., 2004). Similarly, nuclear accumulation of STAT5 was observed upon LMB treatment in a phosphorylation-independent manner (Zeng et al., 2002), which has strengthened the concept that STATs shuttle between the cytoplasm and the nucleus even in the absence of a cytokine stimulus (Fig. 4.2, upper panel).

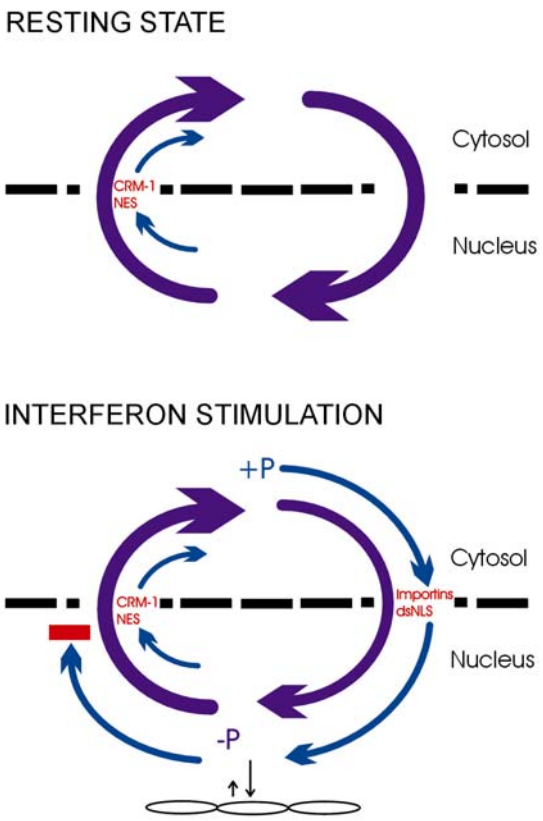


**Fig. 4.2** Schematic representation of STAT1 nucleocytoplasmic shuttling in resting cells (upper panel) and during interferon stimulation (lower panel). Carrier-independent translocation is depicted with purple arrows, carrier-dependent transport with blue arrows. The red bar represents the export block of phosphorylated STAT1 dimers (+P). Dephosphorylation (-P), which is under control of the DNA off-rate (black), is also indicated. Arrow widths are proportionate to the corresponding flux rates (adopted from Vinkemeier, 2004).

It is now well established that STATs continuously shuttle between the cytoplasm and the nucleus in resting cells as well as during cytokine stimulation (Fig. 4.2 and Vinkemeier, 2004; Meyer and Vinkemeier, 2004). Microinjection experiments revealed that the nucleocytoplasmic shuttling of STATs is a rapid, diffusion-controlled process. Nuclear import of unphosphorylated STAT1 after cytoplasmic microinjection was detectable already after 5 min (Marg et al., 2004). Using digitonin-permeabilised cells, we demonstrated that the import and export of unphosphorylated STAT1, STAT3 and STAT5 occurred in the absence of soluble transport factors and metabolic energy (Marg et al., 2004). Moreover, we found that STATs in the non-phosphorylated form can bind to nucleoporins (Marg et al., 2004), and presumably pass the nuclear pore in a carrier-unassisted way, in analogy to importin-β (Yokoya et al., 1999; Koike et al., 2004). Microinjection experiments also revealed that the constitutive shuttling is not affected from the pharmacological inhibition of CRM1 (Meyer et

al., 2002a; Marg et al., 2004). Since in resting cells carrier-mediated import can be neglected, the change in the nucleocytoplasmic distribution of STATs upon export inhibition, therefore reflects the contribution of CRM1-mediated export to STAT localisation in resting cells (Fig. 4.2, upper panel).

As was previously reported by Meyer et al. (2002b), we observed cell type- and STAT-specific differences in the nucleocytoplasmic distribution of the STAT proteins in resting cells. STAT1-GFP is more nuclear in 3T3 cells than in HeLa S3 cells (compare Figs. 3.33A and 3.34A) and GFP-STAT3 is even more nuclear in unstimulated HeLa S3 cells than STAT1 (Figs. 3.33 and Fig. 3.35A). Since both, nucleocytoplasmic shuttling and CRM1-dependent export, proceed at the same time in resting cells, modulation of each transport pathway can account for cell type- and/or STAT-specific differences in the localisation of the proteins. Cell type-specific differences in the nucleocytoplasmic distribution of STATs may be explained by different activities of the nuclear export receptor CRM1 (Meyer et al., 2002b). One possibility is that different expression levels of CRM1 control the nucleocytoplasmic balance of STATs. The export receptor CRM1 is expressed ubiquitously in mammalian cells (Kudo et al., 1997), yet tissue-specific differences in expression have been reported (Holaska and Paschal, 1998). High expression was observed especially in brain, kidney and testes, whereas in heart, lung, muscle, and spleen CRM1 was significantly expressed lower. In addition, tissue-specific co-factors for CRM1 may account for the observed cell type-specific nucleocytoplasmic distribution of STATs.

The differential use of STAT NESs by the export receptor CRM1 is another mechanism that may explain the differences between the localisation of different STATs (McBride and Reich, 2003). Three different NES activities have been reported in STAT1 (Begitt et al., 2000; McBride et al., 2000; Mowen and David, 2000) and the position and number in other family members also varies considerably. Depending on their accessibility, these NESs could operate constitutively and/or conditional. For STAT1 it is well established now that all export activity is masked upon phosphorylation and dimerisation of the protein, since phosphorylated STAT1 is unable to leave the nucleus (Meyer et al., 2003).

The interplay of the different STAT1 NESs, however, still lacks a full characterisation. Direct binding to CRM1 has only been confirmed *in vitro* for the NES in the DNA binding domain of STAT1 (McBride et al., 2002). Another well-studied example is the *Dictyostelium* Dd-STATc, a STAT homologue that has also been shown to translocate into the nucleus independently of tyrosine phosphorylation (Fukuzawa et al., 2003). The nucleocytoplasmic balance of Dd-STATc is determined by the counteracting activities of a transferable import

signal in the N-domain and a constitutive NES (aa 504-554). Accordingly, either deletion of the constitutive NES or its masking following DIF (differentiation-inducing factor) stimulation and phosphorylation-dependent dimerisation led to nuclear accumulation of the transcription factor (Fukuzawa et al., 2003).

Inhibition of STAT nucleocytoplasmic transport turned out to be a strategy that is exploited by several viruses and mycobacteria to escape the host immune system (reviewed in Horvath, 2004). The Nipha virus and the related Hendra virus evade the antiviral activity of alpha and gamma interferons by preventing STAT1 and STAT2 activation and nuclear accumulation (Rodriguez et al., 2002, and 2003). The causative agent has been identified as the V protein of the two paramyxoviruses, which forms high molecular weight complexes with STAT1 and STAT2 in the cytoplasm. Similarly, expression of the HCV (Hepatitis C virus) core protein blocked nuclear accumulation of STAT1 and STAT1 target gene expression (Melen et al., 2004), and impaired nuclear accumulation of STAT4 was reported to occur in patients suffering from recurrent mycobacterial infection (Toyoda et al., 2004). The Nipha V protein, however, not only prevents nuclear accumulation of STAT1 following cytokine treatment but also interferes with the constitutive functions of STAT1. The V protein itself is a shuttling protein and is capable of depleting STAT1 from the nucleus of resting cells (Rodriguez et al., 2002). These initial studies suggest that further analysis of STAT nucleocytoplasmic transport may provide new strategies for therapeutic intervention.